Article

Cell Reports

VEGFR2-Mediated Vascular Dilation as a Mechanism of VEGF-Induced Anemia and Bone Marrow Cell Mobilization

Graphical Abstract

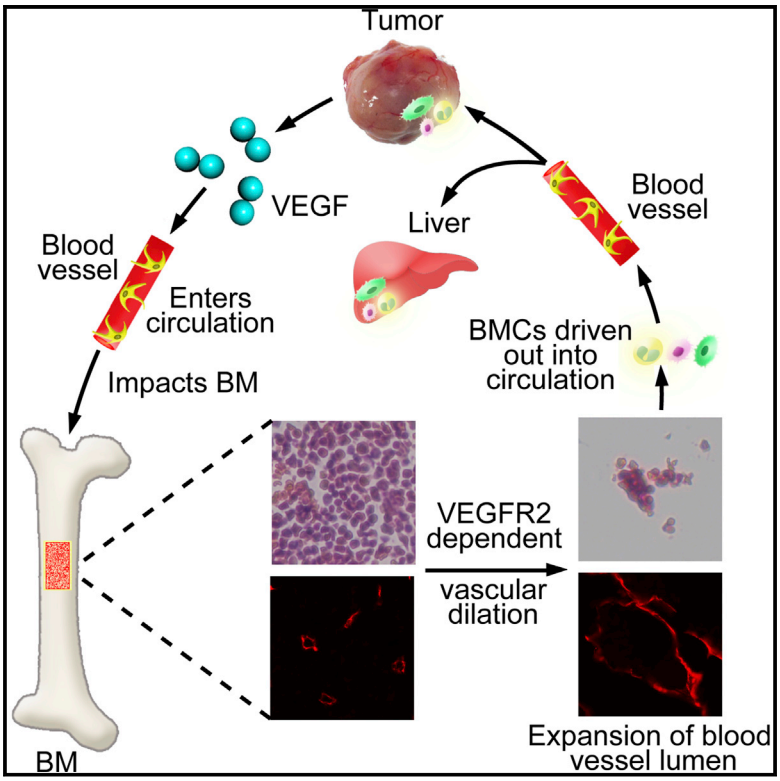

Highlights

Tumor-derived VEGF induces BMC mobilization and vascular dilation

BMC mobilization and vessel dilation is VEGFR2 dependent

Genetic inactivation of VEGFR1 does not affect VEGF-induced BMC mobilization

Endothelial deletion of *Vegfr2* abrogates VEGF-induced BMC mobilization

Authors

Sharon Lim, Yin Zhang, ..., Baocun Sun, Yihai Cao

Correspondence

yihai.cao@ki.se

In Brief

Cancer patients often suffer from cancer cachexia and paraneoplastic syndrome, which significantly impair survival and the quality of life. Here, Lim et al. report that tumor-derived VEGF induces anemia in mice through the mechanism of vessel dilation in bone marrow. The VEGF-VEGFR2-triggered vascular dilation in bone marrow leads to mobilization of bone marrow cells to peripheral tissues and organs. These findings suggest a therapeutic option for treatment of cancer anemia by targeting VEGF-VEGFR2 signaling.

Lim et al., 2014, Cell Reports 9, 569–580
October 23, 2014 ©2014 The Authors
http://dx.doi.org/10.1016/j.celrep.2014.09.003

Cell Reports
Article

VEGFR2-Mediated Vascular Dilation as a Mechanism of VEGF-Induced Anemia and Bone Marrow Cell Mobilization

Sharon Lim,[1,8] Yin Zhang,[1,8] Danfang Zhang,[1,2,8] Fang Chen,[1,3,8] Kayoko Hosaka,[1,8] Ninghan Feng,[1,4,8] Takahiro Seki,[1] Patrik Andersson,[1] Jingrong Li,[5] Jingwu Zang,[5] Baocun Sun,[2,9] and Yihai Cao[1,6,7,9,*]
[1]Department of Microbiology, Tumor and Cell Biology, Karolinska Institute, 171 77 Stockholm, Sweden
[2]Department of Pathology, Tianjin Medical University, 22 Qi Xiang Tai Road, Heping, Tianjin 300070, China
[3]The First Affiliated Hospital of Zhejiang Chinese Medicine University, 54 Youdian Road, Hangzhou, Zhejiang 310006, China
[4]Department of Urology, The Second Hospital of Wuxi, 68 Zhongshan Road, Wuxi, Jiangsu 214002, China
[5]Simcere Pharmaceutical R&D, Nanjing, 699-18 Xuan Wu Avenue, Jiangsu 210042, China
[6]Department of Medicine and Health Sciences, Linköping University, 581 83 Linköping, Sweden
[7]Department of Cardiovascular Sciences, University of Leicester and NIHR Leicester Cardiovascular Biomedical Research Unit, Glenfield Hospital, Leicester LE3 9QP, UK
[8]Co-first author
[9]Co-senior author
*Correspondence: yihai.cao@ki.se
http://dx.doi.org/10.1016/j.celrep.2014.09.003

SUMMARY

Molecular mechanisms underlying tumor VEGF-induced host anemia and bone marrow cell (BMC) mobilization remain unknown. Here, we report that tumor VEGF markedly induced sinusoidal vasculature dilation in bone marrow (BM) and BMC mobilization to tumors and peripheral tissues in mouse and human tumor models. Unexpectedly, anti-VEGFR2, but not anti-VEGFR1, treatment completely blocked VEGF-induced anemia and BMC mobilization. Genetic deletion of *Vegfr2* in endothelial cells markedly ablated VEGF-stimulated BMC mobilization. Conversely, deletion of the tyrosine kinase domain from *Vegfr1* gene ($Vegfr1^{TK-/-}$) did not affect VEGF-induced BMC mobilization. Analysis of $VEGFR1^{+}$/$VEGFR2^{+}$ populations in peripheral blood and BM showed no significant ratio difference between VEGF- and control tumor-bearing animals. These findings demonstrate that vascular dilation through the VEGFR2 signaling is the mechanism underlying VEGF-induced BM mobilization and anemia. Thus, our data provide mechanistic insights on VEGF-induced BMC mobilization in tumors and have therapeutic implications by targeting VEGFR2 for cancer therapy.

INTRODUCTION

In the tumor microenvironment, tumor cells together with other host cellular components including inflammatory cells, stromal fibroblasts, and vascular cells collectively contribute to tumor development, progression, invasion, and metastasis (Hanahan and Weinberg, 2011). Malignant cells and the tumor-infiltrated host cells reciprocally interact with each other. This complex and intimate crosstalk is accomplished through various growth factors, cytokines, and cell-cell interactions. Genetic and epigenetic alterations, as well as microenvironmental changes, often lead to production of various growth factors and cytokines at high levels. Vascular endothelial growth factor (VEGF) is one of the most frequently highly expressed angiogenic factors found in various tumor tissues (Jubb et al., 2004), and its expression level can be further elevated by tissue hypoxia that often exists in solid tumor (Makino et al., 2001). Although VEGF is described as one of the relatively specific endothelial growth factors, it displays broad biological functions by targeting other cell types, including tumor, perivascular, hematopoietic, inflammatory, and neuronal cells (Cao, 2014; Ferrara et al., 2003). These broad tissue effects are determined by the specific distribution of VEGFRs on particular cell types.

VEGF displays its biological functions by activation of its receptors, and it is generally believed that VEGFR2, a cell-surface tyrosine kinase receptor, is the functional receptor that mediates VEGF-induced angiogenesis, vascular permeability, and vascular remodeling (Ferrara et al., 2003; Senger et al., 1983). Conversely, biological functions of VEGFR1-mediated signals remain largely unknown, and it has been suggested that VEGFR1 mediates negative signals that counteract VEGF-induced angiogenesis (Cao, 2009). Based on its relatively broad distribution in various cell types, some of the VEGF-induced non-endothelial activity has been associated with the VEGFR1-signaling system. For example, VEGFR1 is expressed in macrophages and hematopoietic progenitor cells and has been reported to be involved in recruiting these cells to the tumor microenvironment (Cao, 2009). Once these hematopoietic progenitor and inflammatory cells are recruited to the tumor microenvironment, they significantly contribute to tumor

neovascularization. Additionally, VEGF-mobilized bone marrow cells (BMCs) may significantly contribute to cancer metastasis by facilitating malignant cell intravasation and the formation of premetastatic niches in remote organs (Kaplan et al., 2005; Wynn et al., 2013).

In this study, we use several mouse tumor models to study the underlying mechanism by which tumor-derived VEGFs mobilize BMCs. Surprisingly, we found that the mechanism underlying the VEGF-induced BMC mobilization is mediated via VEGFR2-dependent vascular dilation in bone marrow (BM) but independent from VEGFRs expression in BMCs. Thus, targeting endothelial cell VEGFR2, but not VEGFRs in hematopoietic cells, would be an effective approach to inhibit VEGF-stimulated BMCs, which may significantly participate in tumor growth, angiogenesis, and metastasis.

RESULTS

Tumor-Derived VEGF Induces BMC Mobilization, Vascular Dilation, and Permeability

To study the systemic impact of tumor-derived VEGF on BMCs, we established a murine fibrosarcoma (T241) cell line that produces $VEGF_{165}$ (Xue et al., 2008; Yang et al., 2013a; Zhang et al., 2011). Tumor cells were subcutaneously implanted in syngeneic wild-type (WT) C57Bl6 mice, and BM was analyzed when tumor volume reached approximately 1 cm^3 in vector- and VEGF-T241 tumors. The tumor-derived circulating VEGF was detectable in plasma of tumor-bearing mice. The plasma level of VEGF-tumor-bearing mice was significantly higher than that of control tumor-bearing mice (1.2 ng/ml versus 0.06 ng/ml; Figure S1A). Compared with vector-tumor control mice, VEGF-tumor-bearing mice exhibited a severe hematopoietic defect, manifesting robust depletion of BMCs, with an exception of remaining BMCs attached to the bone matrix (Figure 1A). Quantification analysis showed a significant reduction of BMCs in VEGF-tumor-bearing mice relative to controls (Figure 1C). Vascular immunohistochemical staining with endomucin as a sinusoidal endothelial-cell-specific marker (Wang et al., 2013) demonstrated that BM microvessels underwent marked dilation in VEGF-tumor-bearing animals relative to control groups (Figure 1B). Owing to dilation of sinusoidal microvessels in BM, vascular density per field was significantly decreased (Figure 1C). Notably, BM microvessels were also dilated in vector control tumor-bearing mice, although this effect remains relatively modest (Figures 1A–1C). Consistent with BM defects, peripheral red blood cells (RBCs), hemoglobin (HGB), and hematocrit (HCT) in VEGF-tumor-bearing mice were all significantly decreased relative to those of tumor-free healthy mice (Figure S1B).

Similar to $VEGF_{165}$, overexpression of $VEGF_{121}$, a non-heparin-binding soluble VEGF isoform, in tumors also markedly induced BM vessel dilation and BMC loss (Figure S2). In contrast, expression of $VEGF_{189}$, a high-affinity heparin-binding VEGF isoform, did not alter BM vasculatures and BMC mobilization (Figure S2). These findings indicate that non-heparin-binding soluble VEGF molecules are responsible for BM vessel dilation and BMC loss. In contrast to VEGF, overexpression of PlGF and VEGF-B in the same tumor type did not induce vessel dilation and BMC loss (Figure S2). Because PlGF and VEGF-B are VEGFR1 exclusive binding ligands, which lack interactions with VEGFR2, these findings provide independent evidence to further support the VEGFR2-dependent mechanism underlying VEGF-induced BMC loss.

To exclude the possibility that BMC loss was the causal mechanism of BM vessel dilation, we employed irradiation as an alternative approach to induce BMC loss. As expected, irradiation effectively induced BMC loss in mice without causing vessel dilation (Figures 1D and 1E). These findings suggest that BMC loss per se would not significantly alter BM vessel dilation, and VEGF-induced vessel dilation and BMC loss occurred as a sequential event. The other possible mechanism underlying VEGF-induced BMC mobilization is the increase of vascular permeability of BM vasculatures. To study this possibility, large-size rhodamine-labeled 2,000 kDa dextran molecules were injected into tumor-bearing mice. Notably, BM vasculatures of VEGF-tumor-bearing mice showed high permeability of 2,000 kDa dextran whereas BM vasculatures of vector control tumor-bearing mice were completely nonpermeable to these large-size dextran molecules (Figures 1F and 1G). In fact, nearly all injected dextran molecules were extravasated in BM of VEGF-tumor-bearing mice. The highly permeable BM vessels are likely to provide another mechanism of BMC mobilization. Consistent with increased mobilization of BMCs, peripheral blood mononuclear cells (PBMCs) were transiently increased, followed by a decrease (Figure 1H). The fluctuation of white blood cells (WBCs) reflects the dilation-permeability-related mobilization of BMCs and subsequently BM crisis.

VHL Mutation-Induced VEGF in Human Renal Cell Carcinomas Causes BM Vascular Dilation and Anemia

To link our findings to pathophysiological relevance, we studied the impact of tumor-derived VEGF on BM vessels in natural-occurring human tumors. For this reason, we chose a human renal cell carcinoma (768-O RCC-*mut*VHL) with VHL mutations, which often leads to high expression of VEGF due to stabilization of hypoxia-inducible factor-1α (HIF-1α). Reconstitution of *WT*VHL into the 768-O RCC-*mut*VHL enabled us to use the cell line of the same background to study the role of VHL mutation in modulation of BM vascular dilation and BMC mobilization.

The circulating VEGF level of 768-O RCC-*mut*VHL-tumor-bearing mice was high (approximately 500 pg/ml) as compared with that of 768-O RCC-*WT*VHL-tumor-bearing mice (Figure 2A). Consistent with the high-circulating VEGF level, 768-O RCC-*mut*VHL-tumor-bearing mice exhibited suppression of BM hematopoiesis by losing BMCs (Figure 2B). Examination of BM microvessels demonstrated that BM vasculatures became highly dilated, as seen in the mouse tumor models (Figure 2C). The sinusoidal BM microvessels appeared to be disorganized with large and irregular lumen as compared with those of 768-O RCC-*WT*VHL-tumor-bearing mice (Figure 2D). Consistent with BM morphology, 768-O RCC-*mut*VHL-tumor-bearing mice suffered from anemia with reduced RBCs, HGB, and HCT values (Figure 2E). These findings in human renal cell carcinoma (RCC) tumors demonstrate the pathophysiological relevance of our findings and indicate that VHL mutations potentially contribute to development of tumor-associated anemia through the mechanism of VEGF-induced BM vessel dilation.

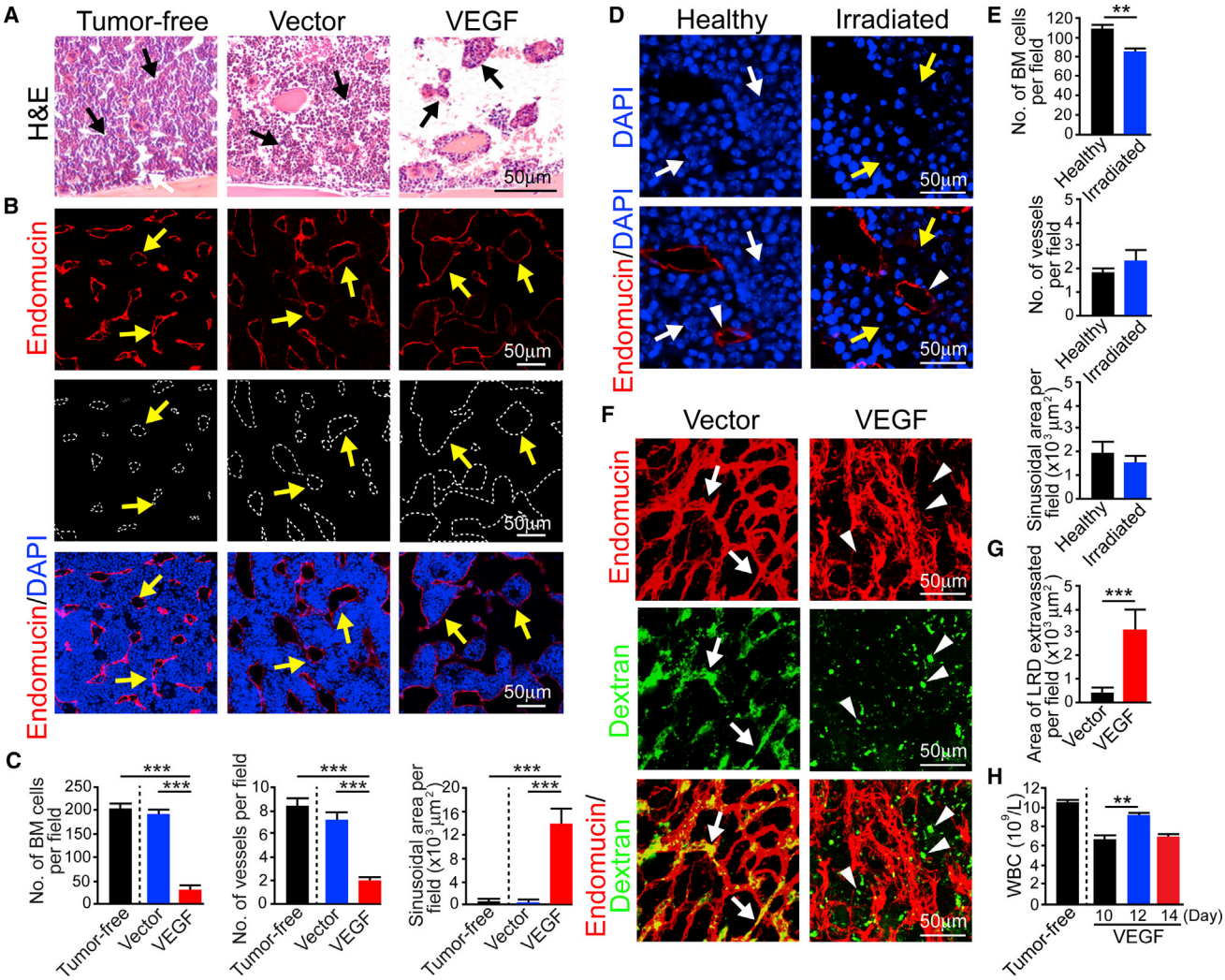

Figure 1. Tumor-Derived VEGF Induces BMC Mobilization and Sinusoidal Vascular Dilation

(A) Hematoxylin and eosin (H&E) staining of BM obtained from the joint region between femur and tibia of tumor-free, vector-, and VEGF-tumor-bearing mice (n = 4–6). Arrows point to BMCs.

(B) Upper panels: endomucin staining of microvessels in BM of tumor-free, vector-, and VEGF-tumor-bearing mice. Lower panels: pseudosimulation of microvessels shown in upper panels. The dash-line-encircled areas show lumens of microvessels. Last panels: endomucin (red) and DAPI (blue) double immunostaining shows the relation between BM microvessels and BMCs. Arrows indicate microvessels.

(C) Quantification of numbers of BMCs, microvessels, and sinusoidal areas of microvessels (n = 6–8).

(D) Irradiated WT C57Bl6 mouse BM was double immunostained with endomucin (red) and DAPI (blue; n = 6). White arrows indicate BMCs, and yellow arrows indicate intercellular distances of irradiated BM. Arrowheads point to microvessels in BM.

(E) Quantification of numbers of BMCs, BM microvessels, and BM vascular sinusoidal areas (n = 6–8).

(F) Perfusion of lysinated 2,000 kDa dextran (green) in BM microvessels that were costained with endomucin (red) of vector- and VEGF-tumor-bearing mice (n = 6). Arrows indicate perfused area (yellow). Arrowheads point to extravasated dextran signals (green).

(G) Quantification of vascular perfusion and extravasated dextran signals (n = 6–8). LRD, lysinated rhodamine dextran.

(H) WBCs from peripheral blood of tumor-free and VEGF tumor-bearing mice were measured (n = 4–6).

The scale bars of each panel represent 50 μm. All data are represented as mean ± SEM. $^{**}p < 0.01$; $^{***}p < 0.001$ (Student's t test; two-tailed). See also Figure S1.

VEGFR2-Dependent Vessel Dilation and BMC Mobilization

We next studied the VEGFR-signaling pathway that mediates microvessel dilation and BMC mobilization. Anti-mouse VEGFR1- and VEGFR2-specific neutralizing antibodies (Yang et al., 2013b) were used to block VEGF-triggered functions. Interestingly, VEGFR2-, but not VEGFR1-, specific blockade virtually completely reversed the VEGF-induced BM defect (Figure 3A). The density of BMCs in VEGFR2 blockade-treated tumor-bearing mice reversed to similar levels of healthy and vector tumor controls (Figure 3C). Consistent with BMC recovery, anti-VEGFR2-treated VEGF-tumor-bearing mice showed normalization of BM vessels with substantial reduction of vascular diameters nearly to those seen in control-vector-tumor-bearing

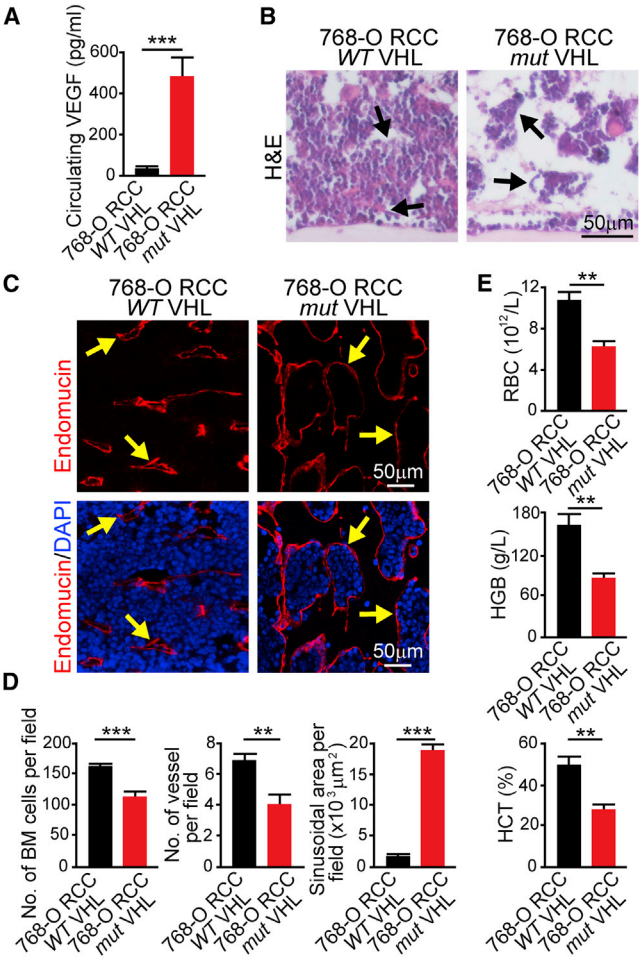

Figure 2. Natural Human-Tumor-Derived VEGF Induces BM Vessel Dilation and Anemia

(A) Circulating levels of VEGF in 768-O RCC-*mut*VHL- and 768-O RCC-*WT*VHL-tumor-bearing mice (n = 5).

(B) H&E staining of BM obtained from femur and tibia of 768-O RCC-*mut*VHL- and 768-O RCC-*WT*VHL-tumor-bearing mice (n = 5). Arrows point to BMCs.

(C) Endomucin staining (red) of microvessels in BM of various groups. Arrows indicate microvascular structures. Endomucin and DAPI (blue) double immunostaining shows the relation between BM microvessels and BMCs. Arrows indicate microvascular structures.

(D) Quantification of numbers of BMCs, numbers of microvessels, and sinusoidal areas of microvessels (n = 6–8).

(E) RBCs, HGB, and HCT from peripheral blood of 768-O RCC-*mut*VHL- and 768-O RCC-*WT*VHL-tumor-bearing mice were measured (n = 5).

The scale bars of each panel represent 50 μm. All data are represented as mean ± SEM. **p < 0.01, ***p < 0.001 (Student's t test; two-tailed).

mice (Figures 3B and 3E). Consequently, microvessel density was significantly increased as measured per field of BM sections (Figure 3D). Similar to VEGFR2 blockade, treatment of VEGF-tumor-bearing mice with an anti-mouse VEGF neutralizing antibody resulted in recovery of BMCs and vascular normalization (Figures 3A–3E). In sharp contrast, treatment with the VEGFR1 blockade did not significantly affect tumor VEGF-induced vessel dilation and BMC mobilization (Figures 3A–3E). To provide further supportive evidence of VEGFR2 activation in endothelial cells, we isolated endothelial cells from BM of VEGF- and vector-tumor-bearing mice. Notably, a substantial amount of VEGFR2 molecules became phosphorylated in BM endothelial cells of VEGF-tumor-bearing mice as compared with those in vector-tumor-bearing mice (Figure 3F). These findings indicate that VEGFR2-mediated signaling is crucial for tumor VEGF-stimulated BMC mobilization.

VEGFR2 Blockade Inhibits BMC Mobilization to Tumor and Peripheral Tissues

To trace mobilization of BMCs to tumor and peripheral tissues, we next performed bone marrow transplantation experiments using BMCs from enhanced GFP (EGFP) mice. In these experimental settings, C57Bl6 syngeneic recipient mice were irradiated, followed by BM transplantation with EGFP$^+$ BMCs from the donor. Xenograft of T241 tumor cells were subcutaneously implanted into recipient mice after 3 weeks of BM transplantation, and tumor-bearing mice were randomly divided into different groups that received various treatments. Consistent with VEGF-induced BMC depletion, tumor-derived circulating VEGF molecules were able to markedly increase mobilization of EGFP$^+$ BMCs to tumor and hepatic tissues relative to that of vector-control tumor-bearing mice (Figures 4A–4C). The increased EGFP$^+$ BMCs to tumor and hepatic tissues were unlikely due to the consequence of increased proliferation of the resident BMCs because these cells were not actively proliferating (Figures 4D and 4E). These findings further validate the fact that circulating VEGF significantly mobilized BMCs to peripheral tissues, resulting in a decreased number of resident cells in BM.

Interestingly, treatment of tumor-bearing recipient mice with the VEGFR2 blockade markedly prevented VEGF-induced mobilization of BMCs to tumors and liver (Figures 4A–4C), supporting the critical role of VEGFR2 in mediating mobilization of BMCs to peripheral tissues. Likewise, a VEGF-specific blockade produced a similar inhibitory effect on BMC mobilization in tumor and liver (Figures 4A–4C). Again, VEGFR1 blockade had no effect on mobilization of EGFP$^+$ BMCs to tumor and liver. These findings further support the fact that VEGFR2-, but not VEGFR1-, mediated signals are essential for BMC mobilization in our tumor models.

Reversible Recovery of Hematopoiesis and Microvasculature after Tumor Removal

Because VEGFR1 and VEGFR2 are expressed in subsets of hematopoietic cells and WBCs (Kumar et al., 2003; Lyden et al., 2001), it is possible that pharmacological interference with VEGFR1 and VEGFR2 blockades would affect BMC production under physiological conditions. It is also highly possible that VEGF plays a crucial role in maintenance of BM microvasculatures. Thus, the effects of anti-VEGFR1 and anti-VEGFR2 treatments in our tumor models could be due to their direct impact on BMCs and microvasculatures, which were not influenced by tumors. To exclude these possibilities, we treated tumor-free healthy mice with VEGFR1 and VEGFR2 blockades. Notably, neither VEGFR1 nor VEGFR2 blockades produced any significant effects on the total

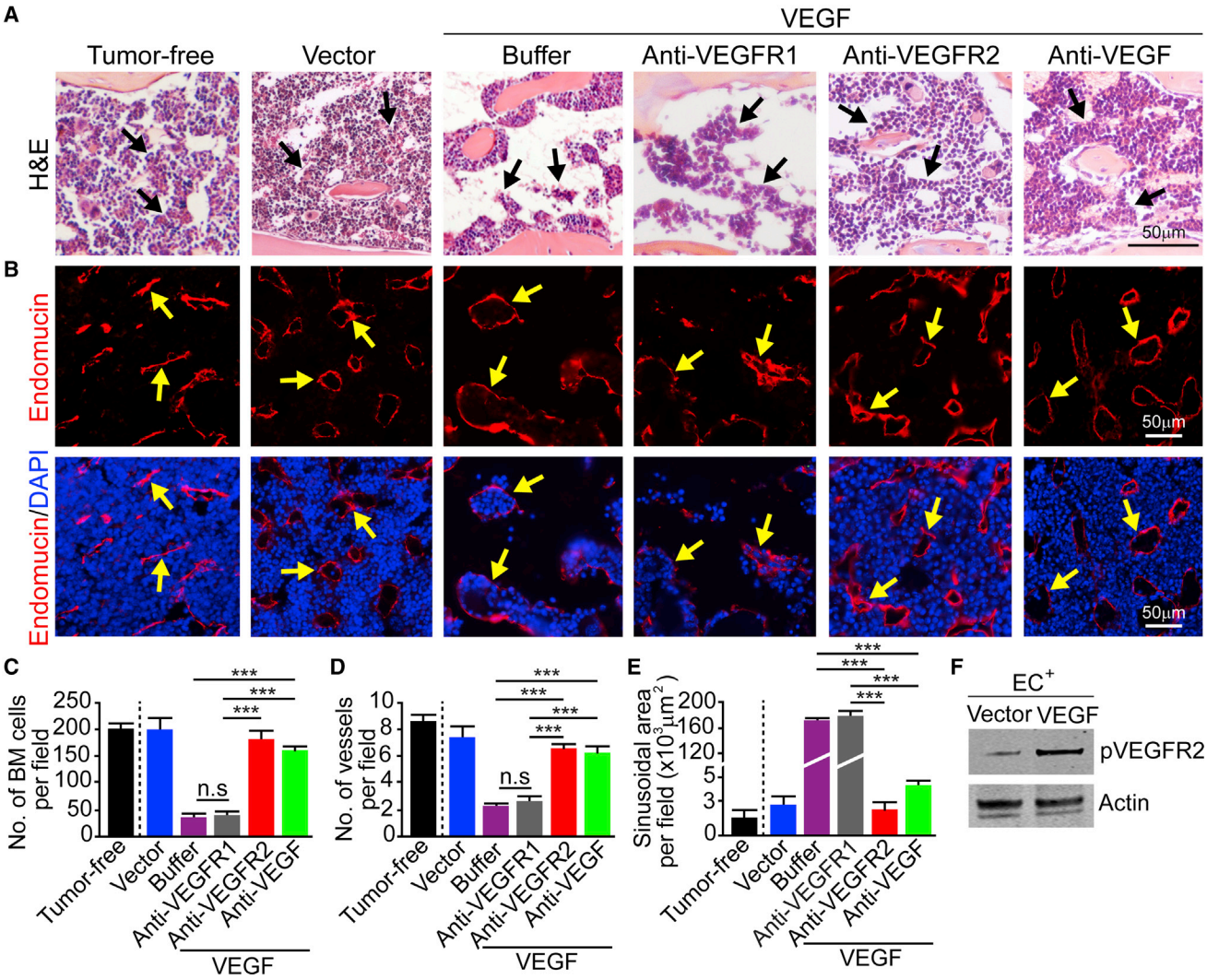

Figure 3. VEGFR2 Blockade Inhibits Circulating VEGF-Induced BM Vascular Dilation and BMC Depletion

(A) H&E staining of vehicle-, anti-VEGFR1-, and anti-VEGFR2-treated and nontreated BM from VEGF-tumor-bearing mice (n = 6). BMs from tumor-free and vector-tumor-bearing mice served as controls. Arrows point to BMCs.

(B) Endomucin (red) and DAPI (blue) double immunostaining shows the relation between BM microvessels and BMCs. Arrows indicate microvascular structures.

(C–E) Quantification of numbers of BMCs (C), numbers of microvessels (D), and sinusoidal areas of microvessels (E). n = 6–8; ns, not significant.

(F) Detection of phosphorylated VEGFR2 by western blot in endothelial cells of BM isolated from vector- and VEGF-tumor-bearing mice. Actin was used for standard loading.

The scale bars of each panel represent 50 μm. All data are represented as mean ± SEM. ***$p < 0.001$ (Student's t test; two-tailed). See also Figure S2.

BMC population, microvessel density, and vascular dilations (Figure S3A).

To study if tumor-derived VEGF-induced BMC depletion and vascular dilation were reversible, we next performed experiments by removing primary tumors in mice that had already developed severe BM phenotypes. Expectedly, BMCs and BM microvessels were almost completely recovered after only 2-week tumor removal (Figure S3B). These findings further demonstrate that tumor-derived VEGF is primarily responsible for causing the BM phenotype. To further study if tumor-removal-recovered BMCs and microvasculatures were dependent on VEGF, three groups of mice, upon resection of primary tumors, were treated with VEGFR1, VEGFR2, and VEGF blockades, respectively. Interestingly, all three anti-VEGF agents had no effects on BMC and microvasculature recovery after removing primary tumors (Figure S3C).

Genetic Inactivation of VEGFR1 Does Not Affect VEGF-Induced BMC Mobilization

In addition to pharmacological interference, we next studied the role of VEGF-induced BMC mobilization and vascular dilation in *Vegfr1*$^{TK-/-}$ mice that only carry the tyrosine-kinase-deleted *Vegfr1* gene (Hiratsuka et al., 1998; Yang et al., 2013a). Stimulation of WT cells including endothelial

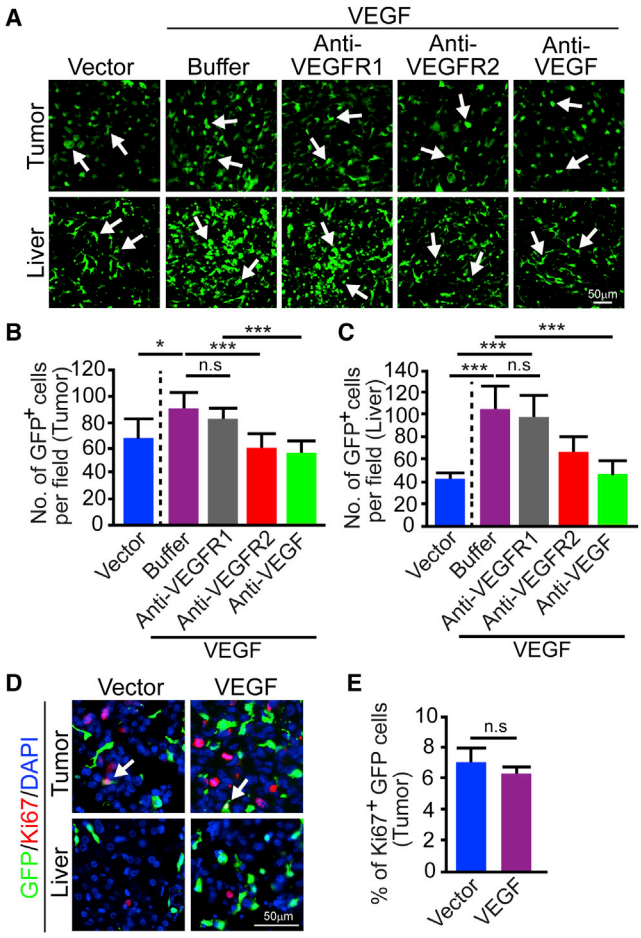

Figure 4. Effects of VEGF, VEGFR1, and VEGFR2 Blockades on Mobilization of Transplanted EGFP$^+$ BMCs

(A) Infiltration of EGFP$^+$ BMCs in tumors and livers of BM-transplanted VEGF-tumor-bearing mice that received treatment of VEGF-, VEGFR1-, and VEGFR2-specific blockades (n = 6–8). Vector tumor bearing was used as control (n = 6–8). Arrows indicate EGFP$^+$ BMCs.

(B and C) Quantification of numbers of EGFP$^+$ BMCs in tumors (B) and in livers (C) of each group (n = 6–8). ns, not significant.

(D) Ki67 (red) and DAPI (blue) double immunostaining of infiltrated EGFP$^+$ BMCs in tumors and livers of BM-transplanted vector- and VEGF-tumor-bearing mice (n = 6–8). Arrows indicate Ki67$^+$-EGFP$^+$ BMCs. ns, not significant.

(E) Quantification of the percentage of Ki67$^+$-proliferative EGFP BMCs (n = 6–8).

The scale bars of each panel represent 50 μm. All data are represented as mean ± SEM. *p < 0.05; ***p < 0.001 (Student's t test; two-tailed). See also Figure S3.

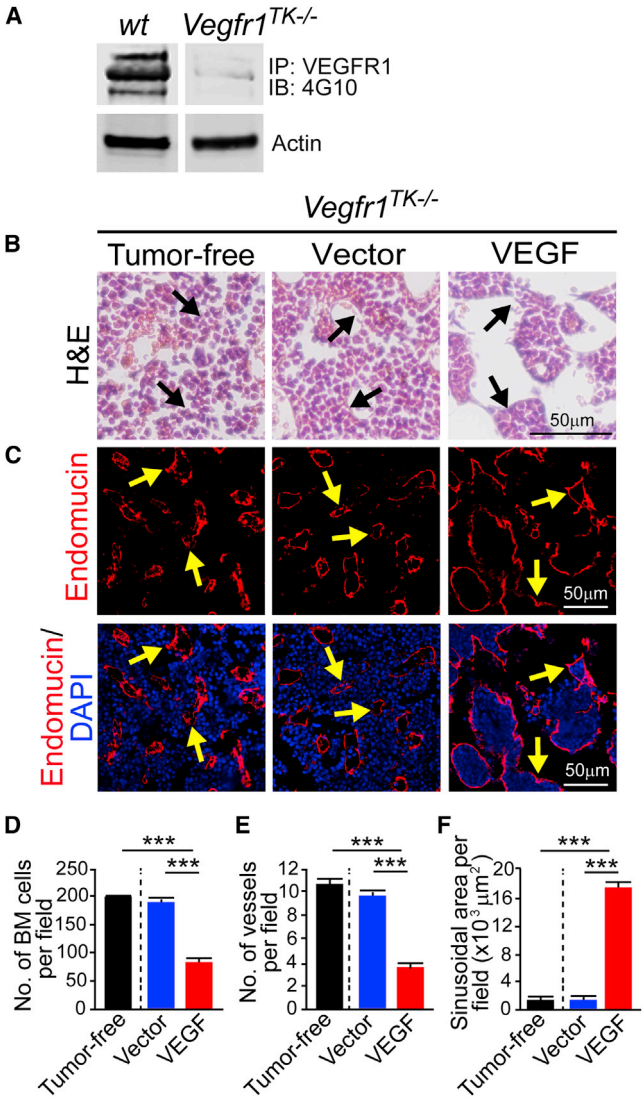

Figure 5. Tumor VEGF-Induced Mobilization of BMCs and Sinusoidal Vascular Dilation in *Vegfr1*$^{TK-/-}$ Mice

(A) Western blot detection of phosphorylation of VEGFR1 by VEGF in cells isolated from BM of WT and *Vegfr1*$^{TK-/-}$ mice. Actin was used for standard loading. IB, immunoblot; IP, immunoprecipitation.

(B) H&E staining of BM of tumor-free, vector-tumor-bearing, and VEGF-tumor-bearing *Vegfr1*$^{TK-/-}$ mice (n = 6). Arrows point to BMCs.

(C) Endomucin staining of microvessels in BM of tumor-free, vector-tumor-bearing, and VEGF-tumor-bearing *Vegfr1*$^{TK-/-}$ mice. Arrows indicate microvascular structures. Endomucin (red) and DAPI (blue) double immunostaining shows the relation between BM microvessels and BMCs. Arrows indicate microvascular structures.

(D–F) Quantification of numbers of BMCs (D), numbers of microvessels (E), and sinusoidal areas of microvessels (F). n = 6–8.

The scale bars of each panel represent 50 μm. All data are represented as mean ± SEM. ***p < 0.001 (Student's t test; two-tailed). See also Figure S4.

cells isolated from BM resulted in phosphorylation of VEGFR1 (Figure 5A). However, VEGFR1 activation was abolished in VEGF-stimulated *Vegfr1*$^{TK-/-}$ BM (Figure 5A). These results validate the defective VEGFR1 signaling in *Vegfr1*$^{TK-/-}$ mice. Intriguingly, tumor VEGF-induced BMC mobilization and BM vascular dilation were not affected in *Vegfr1*$^{TK-/-}$ mice as compared with their littermates (Figures 5B–5F). In fact, the VEGF-induced BM phenotypes were virtually indistinguishable in *Vegfr1*$^{TK-/-}$ mice as compared with those of WT mice (Figures 1A–1C). Similarly, values in peripheral blood including RBCs, HCT, HGB, and WBCs in tumor-bearing and non-tumor-bearing *Vegfr1*$^{TK-/-}$ mice were virtually identical to those seen in WT mice (Figure S1C). These findings further

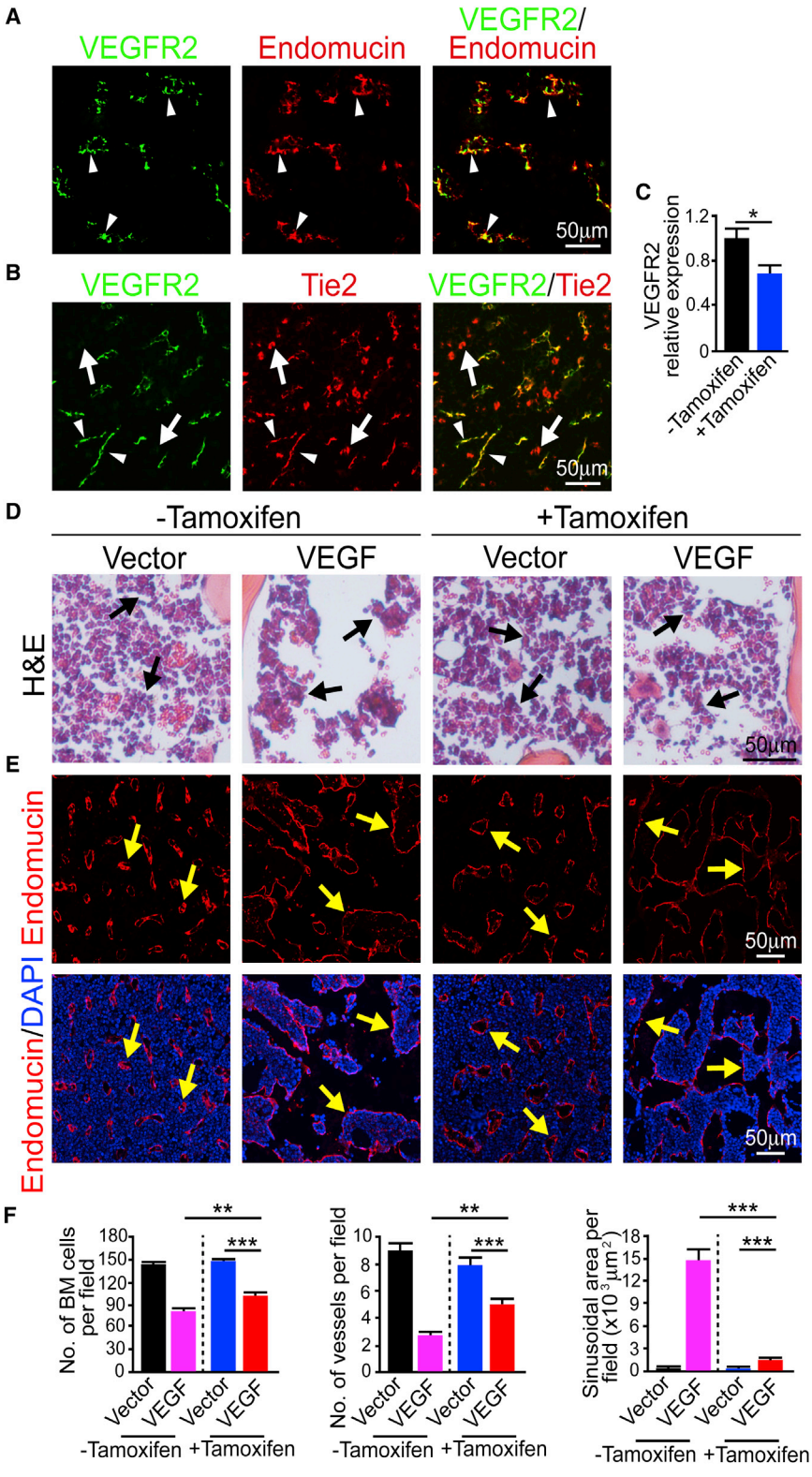

Figure 6. Tumor VEGF-Induced Mobilization of BMCs and Sinusoidal Vascular Dilation in *Vegfr2*$^{lox/lox}$*Tie2*^{CreERT} Mice

(A) VEGFR2 and endomucin double immunostaining of BM. Arrowheads point to VEGFR2 and endomucin double-positive signals.

(B) VEGFR2 and Tie2 double immunostaining of BM. Arrowhead points to VEGFR2 and Tie2 double-positive BM microvessels. Arrows indicate Tie2 positive nonendothelial-cell signals.

(C) Quantification of *Vegfr2* mRNA expression in BM of tamoxifen-treated and nontreated tumor-free *Vegfr2*$^{lox/lox}$*Tie2*^{CreERT} mice (n = 6).

(D) H&E staining of BM of tamoxifen-treated and nontreated vector-tumor-bearing and VEGF-tumor-bearing *Vegfr2*$^{lox/lox}$*Tie2*^{CreERT} mice. Arrows point to BMCs.

(E) Endomucin staining of microvessels in BM of tamoxifen-treated and nontreated vector-tumor-bearing and VEGF-tumor-bearing *Vegfr2*$^{lox/lox}$*Tie2*^{CreERT} mice. Arrows indicate microvascular structures. Endomucin (red) and DAPI (blue) double immunostaining shows the relation between BM microvessels and BMCs. Arrows indicate microvascular structures.

(F) Quantification of numbers of BMCs, numbers of microvessels, and sinusoidal areas of microvessels (n = 6–8).

The scale bars of each panel represent 50 μm. All data are represented as mean ± SEM. **p < 0.01; ***p < 0.001 (Student's t test; two-tailed). See also Figure S5.

Endothelial Deletion of *Vegfr2* Abrogates VEGF-Induced BMC Mobilization

Knowing that VEGFR2 was the crucial receptor for VEGF-induced BMC mobilization, we investigated the in-depth mechanism that underlies VEGF-induced BMC mobilization. A tamoxifen-inducible *Tie2*^{CreERT} mouse strain was crossed with *Vegfr2*$^{lox/lox}$ (Sato et al., 2011) to generate conditional *Vegfr2*$^{lox/lox}$*Tie2*^{CreERT}-deficient mice in endothelial cells. We first performed localization studies to detect VEGFR2 and Tie2 expression in BM. Notably, VEGFR2 expression was restricted to endothelial cells as costained with the endothelial cell marker endomucin (Figure 6A). However, the Tie2^{+} signals were less specific for BM vasculatures, and nonendothelial-cell-positive signals were also detected (Figure 6B). These Tie2^{+} nonendothelial cells might represent Tie2^{+} monocytes/macrophages as described elsewhere (De Palma et al., 2005). Because VEGFR2 expression was restricted in vascular endothelial cells, crossing *Vegfr2*$^{lox/lox}$ with *Tie2*^{CreERT} would only allow excising *Vegfr2* in endothelial cells. Conditional

strengthen our conclusion that VEGFR2, but not VEGFR1, mediates VEGF-induced BMC depletion and BM vascular changes.

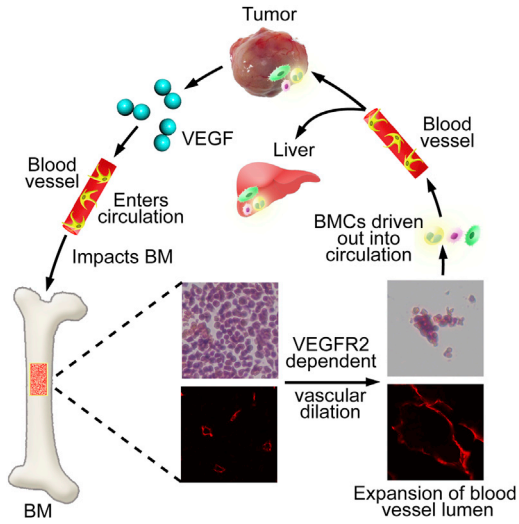

Figure 7. Diagram of Endocrine Functions of Tumor-Derived VEGF
Tumor-derived soluble VEGF enters the circulation and causes sinusoidal dilation of bone marrow microvessels. Vascular dilation of sinusoidal capillaries results in reduced hematopoietic areas and drives out BMCs, leading to an anemic phenotype. VEGF-induced mobilization of BMCs significantly contributes to tumor invasion and metastasis.

Vegfr2$^{lox/lox}$*Tie2*^{CreERT}-deficient mice showed significant reduction of *Vegfr2* mRNA expression (Figure 6C). It should be emphasized that *Vegfr2*$^{lox/lox}$*Tie2*^{CreERT}-deficient mice only showed approximately 30% reduction of VEGFR2 expression. Implantation of VEGF tumors in *Vegfr2*$^{lox/lox}$*Tie2*^{CreERT}-deficient mice significantly abrogated VEGF-induced vascular dilation in BM (Figures 6D–6F). Importantly, BMCs were markedly recovered in VEGF tumor bearing in *Vegfr2*$^{lox/lox}$*Tie2*^{CreERT}-deficient mice, resulting in a normalized hematopoietic phenotype (Figures 6D–6F). In addition, microvessel density was also markedly increased in VEGF tumor bearing in *Vegfr2*$^{lox/lox}$*Tie2*^{CreERT}-deficient mice (Figure 6F). These findings provide compelling evidence that VEGF-induced BM microvessel dilation through the VEGFR2 signaling in endothelial cells is responsible for VEGF-induced BMC mobilization.

Mobilization of VEGFR1- and VEGFR2-Independent BMCs

To study if circulating VEGF preferentially mobilized subpopulations of VEGFR1$^+$ or VEGFR2$^+$ cells, we performed fluorescence-activated cell sorting (FACS) analysis in BM and peripheral blood. To ensure that specific anti-VEGFR1 and anti-VEGFR2 antibodies against mouse were working in our experimental settings, CD31$^+$ endothelial cell fractions from tumor tissues were used as positive controls. As expected, CD31$^+$ endothelial cell fractions showed positive signals in both anti-VEGFR1 and anti-VEGFR2 analyses (Figure S4A). In contrast, a human ovarian cell line completely lacked detectable signals in our FACS analysis (Figure S4A). These findings demonstrate that our anti-VEGFR1- and anti-VEGFR2-based FACS analyses are workable in our experimental settings. Under physiological conditions, VEGFR1$^+$ and VEGFR2$^+$ cells constituted only minor populations of total peripheral blood cells (0.06% VEGFR1$^+$ cells and 0.43% VEGFR2$^+$ cells; Figures S4B–S4D). In vector-tumor-bearing mice, VEGFR1$^+$ and VEGFR2$^+$ cell populations in the peripheral were not significantly altered (0.23% VEGFR1$^+$ cells and 0.22% VEGFR2$^+$ cells; Figures S4B–S4D). Moreover, implantation of VEGF tumors in mice did not dramatically increase the VEGFR1$^+$ and VEGFR2$^+$ cell populations in peripheral blood (0.19% VEGFR1$^+$ cells and 0.47% VEGFR2$^+$ cells; Figure S4B–S4D). These findings demonstrate that tumor-produced circulating VEGF did not alter the percentages of VEGFR1$^+$ and VEGFR2$^+$ cell populations in peripheral blood, implying that active mobilization of these VEGFR$^+$ cells would unlikely be the mechanism underlying the robust effect of VEGF-induced mobilization. It should be emphasized that VEGFR1$^+$ plus VEGFR2$^+$ under all conditions only constituted only <1% of the total nuclear$^+$ cell population in peripheral blood. Thus, this tiny population cannot account for substantial mobilized cells by circulating VEGF.

Consistent with peripheral ratios of VEGFR1$^+$ and VEGFR2$^+$ cell populations, VEGFR1$^+$ and VEGFR2$^+$ BMC populations were not altered in BM of vector- and VEGF-tumor-bearing mice (Figures S4E–S4G). Again, the total VEGFR1$^+$ and VEGFR2$^+$ BMCs represent only a tiny population (<0.4%) of total BMCs. There were no significant ratio changes in tumor-free, healthy, vector-tumor and VEGF-tumor mice. Similarly, the populations of putative Lin(−)/c-Kit(+)/Sca-1(+) hematopoietic stem cells and CD45$^+$ myeloid cells in BM remained unchanged in tumor-free, healthy, vector-tumor and VEGF-tumor mice (Figure S5). These findings suggest that preferential mobilization of VEGFR$^+$ BMCs is unlikely a mechanism of VEGF-induced BMC depletion and peripheral mobilization.

DISCUSSION

We have recently discovered that tumor-derived circulating VEGF represses bone marrow hematopoiesis by mobilizing BMCs (Figure 7; Xue et al., 2008; Zhang et al., 2011). Consistently, others have also reported that VEGF mobilizes BMCs under various pathological conditions through a possible mechanism of interacting with VEGFRs expressed in BMCs (Shaked et al., 2006). Unlike the restricted expression of VEGFR2 in a limited number of cells, VEGFR1 exhibits relatively broad expression patterns on a variety of cell types including monocytes/macrophages and granulocytes (Cao, 2009). Based on expression of VEGFR1 on certain types of BMCs and infiltration of these cells in tumor tissues, it has been suggested that VEGF is able to mobilize these cells from BM to tumor tissues. Despite this reasonable hypothesis, experimental evidence has been lacking to support selective mobilization of VEGFR1$^+$ BMCs by tumor-derived VEGF. In addition to VEGF, several other factors including angiopoietin1, stroma-derived factor, and granulocyte-colony-stimulating factor have been reported to induce BMC mobilization (Ryan et al., 2010; Youn et al., 2011).

Our present study provides several lines of evidence to exclude a direct role of VEGF in mobilization of specific VEGFR$^+$ BMC populations. These include (1) stochastic depletion of BMCs by circulating VEGF that resulted in only scattered hematopoietic islets being attached to the bone matrix;

(2) VEGF-induced BMCs depletion occurred in large areas of BM but unlikely vaporized only a particular cell population; (3) despite its broad distribution in BMCs, pharmacological and genetic inactivation of VEGFR1 produced no impact on BMC mobilization; (4) cell population analysis demonstrated that the ratio of VEGF-mobilized VEGFR$^+$ and VEGFR$^-$ cells in peripheral blood and tissues remained the same as controls, indicating that mobilization occurred indistinctly on all BMCs; (5) inactivation of VEGFR2, which is expressed in a tiny population of BMCs, could virtually completely block tumor VEGF-induced BMC mobilization; and (6) overexpression of VEGFR1 exclusive binding ligands including PlGF and VEGF-B in tumors did not induce vessel dilation and BMC loss. The compelling evidence provided from these data suggests the existence of alternative mechanisms. Examination of blood vessels, the main VEGFR2$^+$ structural component in BM, showed that BM sinusoidal microvessels became high dilated, and the majority of BM area was replaced by vascular lumen. Tumor-derived circulating VEGF-induced vascular dilation also exists in several other tissues and organs including liver, adrenal gland, thyroid, and pancreas (Cao et al., 2004; Eriksson et al., 2003; Feng et al., 1999; Roberts and Palade, 1995; Yang et al., 2013b). Blood vasculatures in these organs are particularly sensitive to VEGF stimulation, and VEGF is crucial for maintenance of microvessel density (Kamba et al., 2006; Yang et al., 2013b). Hematopoietic organs including BM, liver, and spleen contain sinusoidal capillaries (Kopp et al., 2009) that possess fenestrated endothelium and incomplete basement membrane, which permit RBCs, WBCs, as well protein molecules to pass through. Further dilation of the sinusoidal capillaries in BM by VEGF would facilitate intravasation of BMCs into the circulation. In fact, VEGF-induced dilation of sinusoidal BM vessels is highly permeable to large-molecular-weight dextran. Thus, at least two mechanisms are potentially involved in circulating VEGF-induced BMC depletion: (1) dilation of sinusoidal microvessels and increase of vascular permeability in BM and (2) diminishing hematopoietic niches in BM.

Using both pharmacological and genetic approaches, we have found that tumor-derived VEGF-induced BMC mobilization can be completely blocked by inactivation of VEGFR2, but not VEGFR1. These findings are surprising because VEGFR2 is not prominently expressed in BMCs and our localization study shows VEGFR2 expression is restricted in endothelial cells in BM. Notably, genetic deletion of VEGFR2 in endothelial cells largely impaired circulating VEGF-induced mobilization, indicating that the endothelial VEGFR2 mediates BMC mobilization. Although Tie2 expression is not restricted in endothelial cells, specific expression of VEGFR2 in BM endothelial cells would restrict the *Tie2*^{CreERT} recombinase activity to endothelial cells. Thus, the *Vegfr2*$^{lox/lox}$*Tie2*^{CreERT} system in our experimental model system is rather restricted to endothelial cells in BM. To the best of our knowledge, this unexpected mechanism has not been described for VEGF-induced mobilization of BMCs. Thus, our findings provide mechanistic insights on how BMCs are mobilized by VEGF under many pathological conditions. In addition to VEGF and VEGFR2 inhibitors, it is likely other angiogenesis inhibitors such as NADPH oxidase inhibitors (Bartus et al., 2011; Bhandarkar et al., 2009; Garufi et al., 2014; Munson et al., 2012) could also alleviate VEGF-induced anemia. Despite our evidence-based claims, we cannot exclude other possible mechanisms of VEGF-related BMC mobilization. For example, VEGF has been shown to play an important role in mobilization of circulating endothelial precursor cells without significantly affecting BM vasculatures (Lyden et al., 2001). In MMP9-deficient mice, mobilization of VEGF is impaired, leading to defective mobilization of CD45$^+$ myeloid cells (Du et al., 2008). It is likely that VEGFR1 plays a role in that experimental system. Thus, VEGF-induced BMC cell mobilization may involve complex mechanisms by which different BM cell populations are mobilized by distinct pathways.

Cancer patients, especially those with advanced disease, often suffer from systemic diseases including cancer cachexia and paraneoplastic syndrome. Anemia is one of the most common systemic disorders seen in patients with various types of cancers. Our present findings in mouse tumor models demonstrated that tumor-derived circulating VEGF significantly contributes to tumor-associated hematopoiesis suppression in BM. In fact, these findings are pathophysiologically and clinically relevant. It is known that human tumors often express VEGF at high levels as compared with their healthy tissue counterparts (Jubb et al., 2004). In particular, a subset of human RCC tumor tissues expresses VEGF to an extremely high level due to carrying mutations in the *VHL* gene (Jubb et al., 2004). Functional impairment of VHL leads to stabilization of HIF-1α that transcriptionally upregulates VEGF expression (Maxwell et al., 1999). It is known that a substantial number of human RCC patients suffer from paraneoplastic anemia, exhibiting sinusoidal dilation of vasculatures in multiple tissues and organs (Cao, 2010). For example, an early randomized autopsy study of 45 RCC patients showed that 20% of RCC patients exhibited sinusoidal dilation of liver microvessels (Aoyagi et al., 1989). It is likely that their BM microvessels might also become dilated. In our present study, we show that human tumor cells carrying VHL mutations express high levels of VEGF, which causes sinusoidal dilation of BM microvessels. Interestingly, replacement of the mutated VHL with the *WT*VHL in the same RCC cells completely abrogates VEGF-induced vascular phenotypes in BM, indicating that functionally defective VHL mutations are responsible for high-VEGF expression and vascular phenotypes in other nonmalignant tissues. This finding also implies that functionally defective VHL mutations could potentially predict BM anemia in RCC patients and even anti-VEGF drug responses. In fact, RCC patients remain one of the particular cancer populations that benefit the most from anti-VEGF therapy (Brugarolas, 2007). Thus, our findings are clinically relevant.

VEGF-induced sinusoidal dilation is the mechanism for BM hematopoiesis suppression, and therapeutic interference of the systemic effect would be beneficial for host survival. Given the known fact that tumor tissues contain high numbers of inflammatory cells and other hematopoietic cells that collectively contribute to an invasive phenotype and antiangiogenic drug resistance, our present findings imply that blocking the systemic effect of tumor-derived VEGF would be an important approach for antiangiogenic cancer therapy. In support of this view, in preclinical tumor models, survival improvement has been associated with off-tumor targets of anti-VEGF

drugs. Our findings also indicate that normal structures and architectures of BM microvessels are crucial for sustaining physiological hematopoiesis, and interference of BM capillary structures would lead to severe functional impairment. Taken together, our data uncover yet another complex mechanism by which tumor-derived VEGF manipulates the host tissues for the benefit of tumor growth, invasion, and escaping drug resistance.

EXPERIMENTAL PROCEDURES

Animals

WT C57Bl6 and EGFP transgenic mice at ages of 6–8 weeks old were obtained from the Department of Microbiology, Tumor and Cell Biology, Karolinska Institute. *Vegfr1*$^{TK-/-}$ homozygous mice were obtained from Dr. Shibuya Masabumi (University of Tokyo), *Vegfr*$^{lox/lox}$ mice were obtained from Dr. Guo-Hua Fong (University of Connecticut Health Center) generated by Dr. Sato Thomas (Nara Institute of Science and Technology), and *Tie2*^{creERT} mice were obtained from the European Mouse Mutant Archive Organization generated by Dr. Arnold Bernd. Mice are all bred at the Karolinska Institute. All animal studies were reviewed and approved by the North Stockholm Experimental Animal Ethical Committee.

Cell Culture and Reagents

Murine fibrosarcoma cells (T241) were cultured in Dulbecco's modified Eagle's medium (HyClone) supplemented with 10% fetal bovine serum (HyClone). A rabbit anti-mouse VEGF-neutralizing antibody (BD0801) was obtained from Simcere Pharmaceutical R&D (Yang et al., 2013a, 2013b). An anti-mouse VEGFR1-neutralizing antibody and a rat anti-mouse VEGFR2-neutralizing antibody were obtained from Dr. Zhenping Zhu at ImClone. A rat anti-mouse endomucin antibody was purchased from eBioscience (cat. no. 14-5851-85).

Mouse Tumor Models

Approximately 1 × 10^6 T241 tumor cells in 100 μl PBS were subcutaneously inoculated on the dorsal back of C57Bl6, *Vegfr1*$^{TK-/-}$, or *Vegfr2*$^{lox/lox}$*Tie2*^{CreERT} mice. Both 768-O RCC-*WT*VHL and 768-O RCC-*mut*VHL tumor cells in 100 μl PBS were subcutaneously inoculated in immunodeficient mice. Anti-VEGFR1 and anti-VEGFR2 antibodies were administrated intraperitoneally (i.p.) at a dose of 200 μg/mouse twice a week. The anti-VEGF-neutralizing antibody was i.p. injected at a dose of 100 μg/mouse. Treatment with antibodies started when tumor volume were approximately 0.3 cm^3, and treatment lasted for 2 weeks.

Bone Marrow Transplantation

Femur and tibia bones were dissected from the donor EGFP mice immediately after cervical dislocation. BMCs were flushed out with RPMI medium using 21-gauge needles and filtered through a 70 μm nylon mesh cell strainer. BMCs were collected in a 50 ml falcon tube, centrifuged at 1,500 rpm for 6 min, and resuspended in cold PBS. Recipient mice were irradiated at 900 rad gamma rays. Approximately 1.5 × 10^6 donor BMCs were injected into the lateral tail vein of each recipient mouse.

Immunohistochemistry

Fresh bone samples were fixed in 4% paraformaldehyde at 4°C overnight and washed with PBS before paraffin embedding. The embedded samples were cut (5 μm in thickness) and baked at 60°C overnight. Antigen retrieval was achieved using an unmasking solution (Vector Labs; H3300). Samples were blocked with a blocking buffer (4% goat serum in PBS) at room temperature (RT) for 30 min. A rat anti-mouse endomucin antibody (eBioscience; 1:200 dilution in blocking buffer) was used for incubation at 4°C overnight. A secondary fluorescent-conjugated antibody (goat anti-rat Alexa Fluor 555; Invitrogen; A21434; 1:400 dilution in blocking buffer) was incubated at RT for 1 hr. A rabbit anti-mouse VEGFR2 (T104) antibody (1:100 dilution in blocking buffer) or a rat anti-mouse Tie2 antibody (eBioscience E04662; 1:100 dilution in blocking buffer) were used for incubation at 4°C overnight. Secondary fluorescent-conjugated antibodies (goat anti-rat Alexa Fluor 555; Invitrogen; A21434; 1:400 dilution in blocking buffer) and goat anti-rabbit (Alexa 488; Invitrogen; 1:400 dilution in blocking buffer) were incubated at RT for 1 hr. Slides were mounted with Vectashield (Vector Labs; H-1200). Paraffin-embedded samples were sectioned at a thickness of 5 μm and stained with hematoxylin-eosin as described (Hosaka et al., 2013; Lim et al., 2012; Xue et al., 2010, 2012).

Immunoblotting

Equal amounts of cell lysates were subjected to western blot analysis to detect phosphorylated VEGFR2 by incubation with antibodies against phospho-VEGFR2 (2471; Cell Signaling Technology) was followed by secondary antibody incubation. For analysis of VEGFR1 activation, BMCs were collected from WT and *Vegfr1*$^{TK-/-}$ and stimulated with recombinant VEGF for 15 min prior to lysis. Total lysates were incubated with an anti-VEGFR1 antibody (ImClone) followed by protein A/G Agarose (Santa Cruz Biotechnology; sc-2003) immunoprecipitation. Samples were subjected to western blot analysis with antibodies against total phosphotyrosine (4G10; 05-1050; Millipore) followed by secondary antibodies. β-actin (3700S; Cell Signaling Technology) was used as loading control for all blots. Positive signals were visualized using an Odyssey CLx system (LI-COR).

ELISA

Mouse and human VEGF were detected using commercially available VEGF ELISA kits (R&D Systems). All procedures were performed according to the manufacturer's instructions.

Statistical Analysis

For quantification analysis, data were analyzed using two-tailed Student's t test. *$p < 0.05$; **$p < 0.01$; ***$p < 0.001$.

SUPPLEMENTAL INFORMATION

Supplemental Information includes Supplemental Experimental Procedures and five figures and can be found with this article online at http://dx.doi.org/10.1016/j.celrep.2014.09.003.

AUTHOR CONTRIBUTIONS

Y.C. designed the project and contributed the conceptual ideas with assistance from B.S. S.L., Y.Z., and D.Z. designed and performed most experiments with assistance from F.C., K.H., and N.F. T.S. and P.A. contributed to some experiments. J.L. and J.Z. contributed reagents and intellectual inputs. The manuscript was written by Y.C. and prepared by S.L.

ACKNOWLEDGMENTS

We thank Dr. Arnold Bernd and the European Mouse Mutant Archive organization for providing *Tie2*^{CreERT} mice (EC-FP7-Capacities-Specific-Program-funded EMMA service project) and Dr. Masabumi Shibuya at the University of Tokyo for providing *Vegfr1*$^{TK-/-}$ mice for our study. We thank Drs. Thomas Sato and Guo-Hua Fong for providing *Vegfr2*$^{lox/lox}$ mice. We thank Dr. Susanne Schlisio at the Karolinska Institute for providing 768-O RCC-*WT*VHL and 768-O RCC-*mut*VHL cells. We thank Dr. Rolf A. Brekken at UT Southwestern Medical center for providing VEGFR2, T104 antibody. Y.C.'s laboratory is supported by research grants from the Swedish Research Council, the Swedish Cancer Foundation, the Karolinska Institute Foundation, the Karolinska Institute distinguished professor award, the Torsten Söderbergs Foundation, the Novo Nordisk Foundation, and the European Research Council advanced grant ANGIOFAT (project no. 250021).

Received: February 25, 2014
Revised: July 30, 2014
Accepted: August 28, 2014
Published: October 9, 2014

REFERENCES

Aoyagi, T., Mori, I., Ueyama, Y., and Tamaoki, N. (1989). Sinusoidal dilatation of the liver as a paraneoplastic manifestation of renal cell carcinoma. Hum. Pathol. *20*, 1193–1197.

Bartus, C., Brown, L.F., Bonner, M.Y., and Arbiser, J.L. (2011). High level expression of angiopoietin-2 in human abscesses. J. Am. Acad. Dermatol. *64*, 200–201.

Bhandarkar, S.S., Jaconi, M., Fried, L.E., Bonner, M.Y., Lefkove, B., Govindarajan, B., Perry, B.N., Parhar, R., Mackelfresh, J., Sohn, A., et al. (2009). Fulvene-5 potently inhibits NADPH oxidase 4 and blocks the growth of endothelial tumors in mice. J. Clin. Invest. *119*, 2359–2365.

Brugarolas, J. (2007). Renal-cell carcinoma—molecular pathways and therapies. N. Engl. J. Med. *356*, 185–187.

Cao, Y. (2009). Positive and negative modulation of angiogenesis by VEGFR1 ligands. Sci. Signal. *2*, re1.

Cao, Y. (2010). Off-tumor target—beneficial site for antiangiogenic cancer therapy? Nat Rev Clin Oncol *7*, 604–608.

Cao, Y. (2014). VEGF-targeted cancer therapeutics-paradoxical effects in endocrine organs. Nat. Rev. Endocrinol. *10*, 530–539.

Cao, R., Eriksson, A., Kubo, H., Alitalo, K., Cao, Y., and Thyberg, J. (2004). Comparative evaluation of FGF-2-, VEGF-A-, and VEGF-C-induced angiogenesis, lymphangiogenesis, vascular fenestrations, and permeability. Circ. Res. *94*, 664–670.

De Palma, M., Venneri, M.A., Galli, R., Sergi Sergi, L., Politi, L.S., Sampaolesi, M., and Naldini, L. (2005). Tie2 identifies a hematopoietic lineage of proangiogenic monocytes required for tumor vessel formation and a mesenchymal population of pericyte progenitors. Cancer Cell *8*, 211–226.

Du, R., Lu, K.V., Petritsch, C., Liu, P., Ganss, R., Passegué, E., Song, H., Vandenberg, S., Johnson, R.S., Werb, Z., and Bergers, G. (2008). HIF1alpha induces the recruitment of bone marrow-derived vascular modulatory cells to regulate tumor angiogenesis and invasion. Cancer Cell *13*, 206–220.

Eriksson, A., Cao, R., Roy, J., Tritsaris, K., Wahlestedt, C., Dissing, S., Thyberg, J., and Cao, Y. (2003). Small GTP-binding protein Rac is an essential mediator of vascular endothelial growth factor-induced endothelial fenestrations and vascular permeability. Circulation *107*, 1532–1538.

Feng, D., Nagy, J.A., Pyne, K., Hammel, I., Dvorak, H.F., and Dvorak, A.M. (1999). Pathways of macromolecular extravasation across microvascular endothelium in response to VPF/VEGF and other vasoactive mediators. Microcirculation *6*, 23–44.

Ferrara, N., Gerber, H.P., and LeCouter, J. (2003). The biology of VEGF and its receptors. Nat. Med. *9*, 669–676.

Garufi, A., D'Orazi, V., Arbiser, J.L., and D'Orazi, G. (2014). Gentian violet induces wtp53 transactivation in cancer cells. Int. J. Oncol. *44*, 1084–1090.

Hanahan, D., and Weinberg, R.A. (2011). Hallmarks of cancer: the next generation. Cell *144*, 646–674.

Hiratsuka, S., Minowa, O., Kuno, J., Noda, T., and Shibuya, M. (1998). Flt-1 lacking the tyrosine kinase domain is sufficient for normal development and angiogenesis in mice. Proc. Natl. Acad. Sci. USA *95*, 9349–9354.

Hosaka, K., Yang, Y., Seki, T., Nakamura, M., Andersson, P., Rouhi, P., Yang, X., Jensen, L., Lim, S., Feng, N., et al. (2013). Tumour PDGF-BB expression levels determine dual effects of anti-PDGF drugs on vascular remodelling and metastasis. Nat Commun *4*, 2129.

Jubb, A.M., Pham, T.Q., Hanby, A.M., Frantz, G.D., Peale, F.V., Wu, T.D., Koeppen, H.W., and Hillan, K.J. (2004). Expression of vascular endothelial growth factor, hypoxia inducible factor 1alpha, and carbonic anhydrase IX in human tumours. J. Clin. Pathol. *57*, 504–512.

Kamba, T., Tam, B.Y., Hashizume, H., Haskell, A., Sennino, B., Mancuso, M.R., Norberg, S.M., O'Brien, S.M., Davis, R.B., Gowen, L.C., et al. (2006). VEGF-dependent plasticity of fenestrated capillaries in the normal adult microvasculature. Am. J. Physiol. Heart Circ. Physiol. *290*, H560–H576.

Kaplan, R.N., Riba, R.D., Zacharoulis, S., Bramley, A.H., Vincent, L., Costa, C., MacDonald, D.D., Jin, D.K., Shido, K., Kerns, S.A., et al. (2005). VEGFR1-positive haematopoietic bone marrow progenitors initiate the pre-metastatic niche. Nature *438*, 820–827.

Kopp, H.G., Hooper, A.T., Avecilla, S.T., and Rafii, S. (2009). Functional heterogeneity of the bone marrow vascular niche. Ann. N Y Acad. Sci. *1176*, 47–54.

Kumar, S., Witzig, T.E., Timm, M., Haug, J., Wellik, L., Fonseca, R., Greipp, P.R., and Rajkumar, S.V. (2003). Expression of VEGF and its receptors by myeloma cells. Leukemia *17*, 2025–2031.

Lim, S., Honek, J., Xue, Y., Seki, T., Cao, Z., Andersson, P., Yang, X., Hosaka, K., and Cao, Y. (2012). Cold-induced activation of brown adipose tissue and adipose angiogenesis in mice. Nat. Protoc. *7*, 606–615.

Lyden, D., Hattori, K., Dias, S., Costa, C., Blaikie, P., Butros, L., Chadburn, A., Heissig, B., Marks, W., Witte, L., et al. (2001). Impaired recruitment of bone-marrow-derived endothelial and hematopoietic precursor cells blocks tumor angiogenesis and growth. Nat. Med. *7*, 1194–1201.

Makino, Y., Cao, R., Svensson, K., Bertilsson, G., Asman, M., Tanaka, H., Cao, Y., Berkenstam, A., and Poellinger, L. (2001). Inhibitory PAS domain protein is a negative regulator of hypoxia-inducible gene expression. Nature *414*, 550–554.

Maxwell, P.H., Wiesener, M.S., Chang, G.W., Clifford, S.C., Vaux, E.C., Cockman, M.E., Wykoff, C.C., Pugh, C.W., Maher, E.R., and Ratcliffe, P.J. (1999). The tumour suppressor protein VHL targets hypoxia-inducible factors for oxygen-dependent proteolysis. Nature *399*, 271–275.

Munson, J.M., Fried, L., Rowson, S.A., Bonner, M.Y., Karumbaiah, L., Diaz, B., Courtneidge, S.A., Knaus, U.G., Brat, D.J., Arbiser, J.L., and Bellamkonda, R.V. (2012). Anti-invasive adjuvant therapy with imipramine blue enhances chemotherapeutic efficacy against glioma. Sci. Transl. Med. *4*, 27ra36.

Roberts, W.G., and Palade, G.E. (1995). Increased microvascular permeability and endothelial fenestration induced by vascular endothelial growth factor. J. Cell Sci. *108*, 2369–2379.

Ryan, M.A., Nattamai, K.J., Xing, E., Schleimer, D., Daria, D., Sengupta, A., Köhler, A., Liu, W., Gunzer, M., Jansen, M., et al. (2010). Pharmacological inhibition of EGFR signaling enhances G-CSF-induced hematopoietic stem cell mobilization. Nat. Med. *16*, 1141–1146.

Sato, W., Tanabe, K., Kosugi, T., Hudkins, K., Lanaspa, M.A., Zhang, L., Campbell-Thompson, M., Li, Q., Long, D.A., Alpers, C.E., and Nakagawa, T. (2011). Selective stimulation of VEGFR2 accelerates progressive renal disease. Am. J. Pathol. *179*, 155–166.

Senger, D.R., Galli, S.J., Dvorak, A.M., Perruzzi, C.A., Harvey, V.S., and Dvorak, H.F. (1983). Tumor cells secrete a vascular permeability factor that promotes accumulation of ascites fluid. Science *219*, 983–985.

Shaked, Y., Ciarrocchi, A., Franco, M., Lee, C.R., Man, S., Cheung, A.M., Hicklin, D.J., Chaplin, D., Foster, F.S., Benezra, R., and Kerbel, R.S. (2006). Therapy-induced acute recruitment of circulating endothelial progenitor cells to tumors. Science *313*, 1785–1787.

Wang, L., Benedito, R., Bixel, M.G., Zeuschner, D., Stehling, M., Sävendahl, L., Haigh, J.J., Snippert, H., Clevers, H., Breier, G., et al. (2013). Identification of a clonally expanding haematopoietic compartment in bone marrow. EMBO J. *32*, 219–230.

Wynn, T.A., Chawla, A., and Pollard, J.W. (2013). Macrophage biology in development, homeostasis and disease. Nature *496*, 445–455.

Xue, Y., Religa, P., Cao, R., Hansen, A.J., Lucchini, F., Jones, B., Wu, Y., Zhu, Z., Pytowski, B., Liang, Y., et al. (2008). Anti-VEGF agents confer survival advantages to tumor-bearing mice by improving cancer-associated systemic syndrome. Proc. Natl. Acad. Sci. USA *105*, 18513–18518.

Xue, Y., Lim, S., Bråkenhielm, E., and Cao, Y. (2010). Adipose angiogenesis: quantitative methods to study microvessel growth, regression and remodeling in vivo. Nat. Protoc. *5*, 912–920.

Xue, Y., Lim, S., Yang, Y., Wang, Z., Jensen, L.D., Hedlund, E.M., Andersson, P., Sasahara, M., Larsson, O., Galter, D., et al. (2012). PDGF-BB modulates hematopoiesis and tumor angiogenesis by inducing erythropoietin production in stromal cells. Nat. Med. *18*, 100–110.

Yang, X., Zhang, Y., Yang, Y., Lim, S., Cao, Z., Rak, J., and Cao, Y. (2013a). Vascular endothelial growth factor-dependent spatiotemporal dual roles of placental growth factor in modulation of angiogenesis and tumor growth. Proc. Natl. Acad. Sci. USA *110*, 13932–13937.

Yang, Y., Zhang, Y., Cao, Z., Ji, H., Yang, X., Iwamoto, H., Wahlberg, E., Länne, T., Sun, B., and Cao, Y. (2013b). Anti-VEGF- and anti-VEGF receptor-induced vascular alteration in mouse healthy tissues. Proc. Natl. Acad. Sci. USA *110*, 12018–12023.

Youn, S.W., Lee, S.W., Lee, J., Jeong, H.K., Suh, J.W., Yoon, C.H., Kang, H.J., Kim, H.Z., Koh, G.Y., Oh, B.H., et al. (2011). COMP-Ang1 stimulates HIF-1α-mediated SDF-1 overexpression and recovers ischemic injury through BM-derived progenitor cell recruitment. Blood *117*, 4376–4386.

Zhang, D., Hedlund, E.M., Lim, S., Chen, F., Zhang, Y., Sun, B., and Cao, Y. (2011). Antiangiogenic agents significantly improve survival in tumor-bearing mice by increasing tolerance to chemotherapy-induced toxicity. Proc. Natl. Acad. Sci. USA *108*, 4117–4122.